16th World Conference on Earthquake, 16WCEE 2017
Santiago Chile, January 9th to 13th 2017
Paper N° 4040
Registration Code: S-B1460541825

ROCKING ISOLATION OF BRIDGE PIERS USING ELASTOMERIC PADS

M. Titirla[(1)], N. Zarkadoulas[(2)], S. Mitoulis[(3)] and G. Mylonakis[(4)]

[(1)] Dr Civil Engineer, Aristotle University of Thessaloniki, Greece mtitirla@civil.auth.gr
[(2)] Civil Engineer MSc, University of Surrey, United Kingdom nz00077@surrey.ac.uk
[(3)] Assistant Professor, University of Surrey, United Kingdom, s.mitoulis@surrey.ac.uk, www.mitoulis.com
[(4)] Professor, Chair in Geotechnics and Soil-Structure Interaction, University of Bristol, United Kingdom & Professor, University of Patras, Greece, g.mylonakis@bristol.ac.uk

Abstract

Bridge rocking isolation has attracted the interest of the bridge engineering community, as it minimises damage in the structural system, which conforms to the objectives for resilient and sustainable bridges. Two fundamentally different approaches have emerged in recent years: (a) ***structural rocking isolation***, where the piers (cast-in-situ or precast with/without post-tensioning and/or dissipaters) are allowed to rock and minimise damage and (b) ***geotechnical rocking isolation***, where conventionally designed or deliberately under-designed foundations rock to achieve the same goal. However, both structural rocking and rocking footings are facing challenging design aspects. Structural rocking seems to include post-tensioned partially stressed tendons, dissipators and replaceable, internal or external, rebars. Low dissipation capacity and increased on-site labour seem to be the main acknowledged barriers to the application of structural rocking. On the other hand, bridge piers with rocking footings appear to suffer from excessive settlements and, in some cases, large residual drifts, due to the sinking/tilting effect of footings in yielding foundation soils.
Aiming to achieve a simpler rocking mechanism, this paper studies bridge piers isolated by rocking footings, which are deliberately under-designed, yet supported on elastomeric pads. The pier footing rocks on the elastomer and tends to uplift. The pads dissipate energy, whilst exhibit minimal residual drifts. The pier, the footing and the elastomeric pad are supported on an appropriately designed rigid concrete sub-base to achieve minimal settlements. Assessment of the rocking system is based on the response of rocking piers modelled in ABAQUS.

Keywords: bridge, pier, rocking isolation; elastomeric pads

1. Introduction

An urgent challenge for the transportation networks has been placed worldwide with regard to adaptation of deficient bridges to increased traffic needs and natural hazards [1] including earthquake excitations. Efficient and rapid upgrading of bridges is possible when the design prescribes minimal damages and accounts for potential upgrades on the basis of structural resilience i.e. rapid restoration and adaptation. With more than 300000 bridges in Europe having a total value of around 50 billion Euros, a moderate 2% increase in load capacity or residual life, would result in savings of the order of 1 billion Euros. Indicatively, the cost for retrofitting a small size bridge pier with traditional methods, e.g. steel jackets, has been estimated at 52k Euros [2]. Thus, resilient bridge designs that can adapt to increased loading requirements will provide significant cost-savings. Additionally, the end-user society is now demanding much more from infrastructures. Societies expect accelerated constructions, expeditious reconstructions, minimal damage and rapid upgrading for bridges. The latter is anticipated despite the fact that conventional designs prescribe damages on bridge piers [3]. Also, design guidelines do not prescribe bridge resilience, i.e. minimal damage and versatility, and this is an acknowledged gap [4]. In the absence of prolepsis for structural adjustments and adaptation, the restoration of the existing bridge stock is very expensive, time consuming and causes extended disruptions. Thus, a paradigm shift is required to provide damage-free bridges and rapid restoration times.

Bridge isolation and in particular rocking isolation based on accelerated bridge construction principles, comprise a unique philosophy which can provide damage-free bridges [4]. Structural designs based on rocking

isolation can provide minimal damage and higher robustness of functionality, as the sacrificial members can be replaced easily and quickly. It is only in the last decade that rocking isolation was given full consideration in bridges [5-8]. Structural and geotechnical rocking are the two approaches in the international literature. Structural rocking is based on the rocking of bridge piers. In structural rocking, the energy dissipation occurs due to the contact effects of the rocking components. However, it is widely recognized that there is an urgent need for simplifying the connections and for improving energy dissipation of rocking piers. On the other hand, foundation rocking, is based on the uplift of the footings, where the main source of energy dissipation is the yielding of the soil. However, large potential soil settlements and residual tilting impede its application in practice [9-10].

This paper proposes a new design of rocking bridge piers using elastomeric pads. In particular the pier is supported on a deliberately under-designed footing. Three different pier designs were preliminarily designed under certain design criteria and modelled on ABAQUS [11]: (a) a pier model fixed at its base; (b) a pier on a rocking footing and supported on a concrete sub-base and (c) a pier footing rocking on an appropriately designed elastomeric pad. The model piers were then analysed for seven acceleration time histories corresponding to the real earthquake records. The latter two models have the same footing dimensions, whilst the first one employs a pile foundation, which is typically considered to provide fixity to the pier base. Geometric and material non-linearities are taken into consideration. The pier, which rocks on high damping elastomeric pads, was found to efficiently dissipate energy without developing damage observed in the conventional fixed pier. Also, rocking on an elastomeric pad provides efficient means for controlling the axial load on the pier, which was found to exhibit significant fluctuations when the footing was allowed to rock on the concrete sub-base. Also, the use of a high-damping pad reduces drastically the potential sliding and permanent dislocations of the piers as well as the permanent rotations and drifts due to rocking.

2. Description of the piers and FE modeling

Three different pier models were modelled in detail and subjected to earthquake excitations. The pier models have heights of 10 m. The attributed mass of the deck corresponding to a length of 35 m of the superstructure was considered. The attributed deck mass of 850 Mg takes into account the self-weight of the deck, additional permanent and 20% of the variable i.e. traffic loads. The weight of the pier and footing was also taken into account considering self-weight of 25kN/m^3 for reinforced concrete. Fig. 1a shows the longitudinal section of the pier, the attributed deck length, the footing, the elastomeric pad and the concrete sub-base, whilst Fig. 1b shows the foundation plan. The dimensions of the pier 1.0 x 4.0 m correspond to a typical wall-type bent. The analyses presented herein refer to the longitudinal direction of the bridge. The footing was deliberately under-designed to promote rocking of the pier. The dimension of the footing is 3.0 x 5.0 m. The design of the footing was based on criteria to minimise the permanent compressive strain of the elastomeric pad under the vertical loads (i.e. construction stage and serviceability), to rectify the permanent dislocation (sliding) of the footing and to limit the potential uplift of the foundation so that the effective area of the foundation could be at least 2/3 of the actual area for all the design cases examined here. Also, the bearing compressive stresses were checked for the serviceability loads (self-weight of the structure) and for the maximum footing rotations and pier drifts. The initial pressure of the pad under the self-weight of the bridge deck and pier was approximately 0.68 MPa, whilst the pad is subjected to a maximum pressure of 1.66 MPa when the pier drift was approximately 3%, that is significantly smaller than the normal pressure that elastomeric bearings are expected to receive when subjected to seismic excitations. It is noted that the pressure of steel-laminated elastomeric bearings for serviceability design situations ranges between 5 and 10 MPa. Different dimensions were analysed for variable pier drifts ranging from 1.0% to 5.0%. Also, alternative elastomeric pad properties and designs (soft and hard elastomeric pads with or without reinforcing steel plating) were examined during the preliminary design of the pier models. Further details on the design of the footing and the pad are given in the following section. The sliding of the pier footing is restricted along the two horizontal directions by a recess that is formed by the concrete sub-base. In addition, the footing is free to move only along z axis. Appropriate design of the pier footing allows for unrestrained footing rocking and restricting horizontal movements only. The deck was not modelled. The pier top was considered to be monolithically connected to the deck. Evidence is provided elsewhere [12] that the aforementioned pier-deck connection practically restricts the rotations of the pier top. Hence, the pier top is free

to move along x, y and z axes, but the RY rotations about the transverse axis is restrained at all cases to account for pier fixity. The latter simplification was checked and it was found to be accurate under the assumption that the deck is prestressed and thus uncracked. With regard to bottom boundary conditions, the three models investigated are the fully-fixed (FX) one, the model with the footing that rocks on the concrete sub-base thus a concrete to concrete (CC) rocking is promoted, and the model pier with a footing that rocks on the appropriately designed high-damping elastomeric pad, thus a controllable concrete to pad (CP) rocking is promoted.

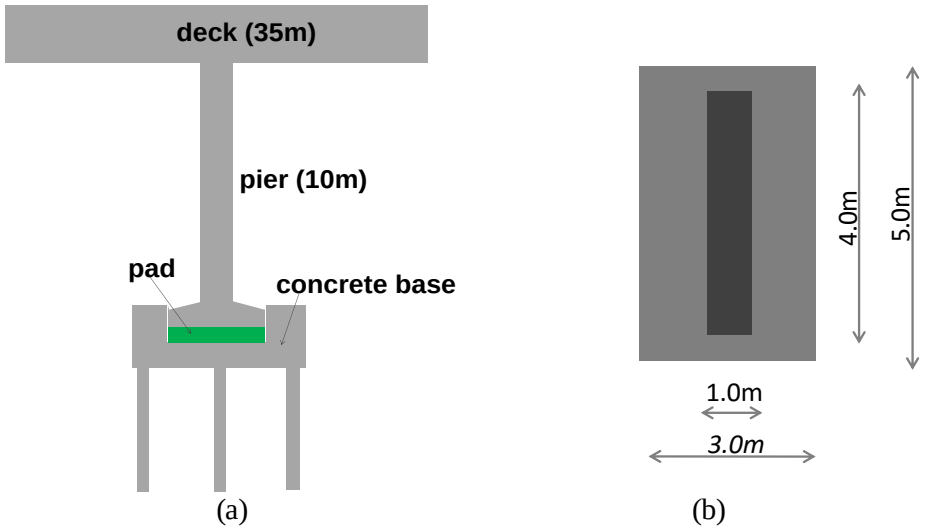

Fig. 1 – Description of the pier: (a) longitudinal section and, (b) plan of the foundation and the pier.

The general purpose FE software ABAQUS ver. 10.1 was employed to simulate the behavior of the three pier models described above i.e. FX, CC and CP. Implicit non-linear dynamic time history analysis was chosen as it permits the handling of very general contact conditions for complicated contact effects, without generating numerical instabilities. For the dynamic analysis, 3D reduced integration solid elements were used. Reduced integration decreases the number of constraints introduced by an element when there are internal constraints in the continuum theory being modelled, if solid elements are used to analyse interaction problems. In such applications fully integrated elements will "lock" and will exhibit response that is orders of magnitude too stiff. The reduced-integration version of the same element was found to provide more efficient modelling for this research [11].

The footing and the elastomeric pad were modelled by 3d solid homogeneous sections and were suitably meshed by using the 3d reduced integration solid element C3D8R (eight-node bricks). The model has a fine meshing of 2264 elements for the FX and the CC model, while a total of 3170 elements were used for the CP model, as shown in Fig. 2. Concrete modeled with an elastoplastic material with Young Modulus of 32GPa, yield stress σ_y of 32Mpa, and maximum stress σ_u of 45Mpa. The model of the elastomer that was selected is the Ogden model [13], a hyperelastic model. Its behaviour is nonlinear, elastic and incompressible. The initial values of the parameters concerning the strain energy density function were chosen and calibrated against the Ohsaki et al. model [14]. For the hysteretic parameters of the Ogden model, the values suggested by the ABAQUS manual [15] were used. The values were imported in ABAQUS according to the study made by Bergström & Boyce [16]. The pier was modelled as a beam element, as shown in Fig. 2. The deck mass was assigned as concentrated mass of 850 Mg on the pier top. Total mass of the system, including the pier and the footing is 1018 Mg. After the imposition of the mass, the pressure on the concrete base (CC model) and on the elastomeric pad (CP model) was found to be 0.67 MPa.

The contact conditions between the two surfaces (footing to concrete sub-base and footing to elastomeric pad) are governed by kinematic constraints in the normal and tangential directions. The normal stress at contact areas is either zero, when there is a gap between the two surfaces, or compressive when the surfaces are in contact. When contact is lost (gap>0) the pressure between the surfaces is zero. When the two surfaces are in

contact (gap=0), the overpressure can reach up very high values, but no penetration of one surface into the other is permitted. The contact between the surfaces is defined as a surface-to-surface contact with a finite sliding option. For the sliding of the footing, the Coulomb friction was used as a common model that describes the interaction of surfaces in contact. The model characterises the frictional behaviour between the surfaces using a coefficient of friction, μ. The coefficient of friction between the rubber and the concrete surfaces ranges from 0.6 to 1.2. To model the contact areas in ABAQUS, the surface to surface contact was used with a coefficient of friction equal to μ=0.80 (mean value). The three pier models are shown in Fig. 2.

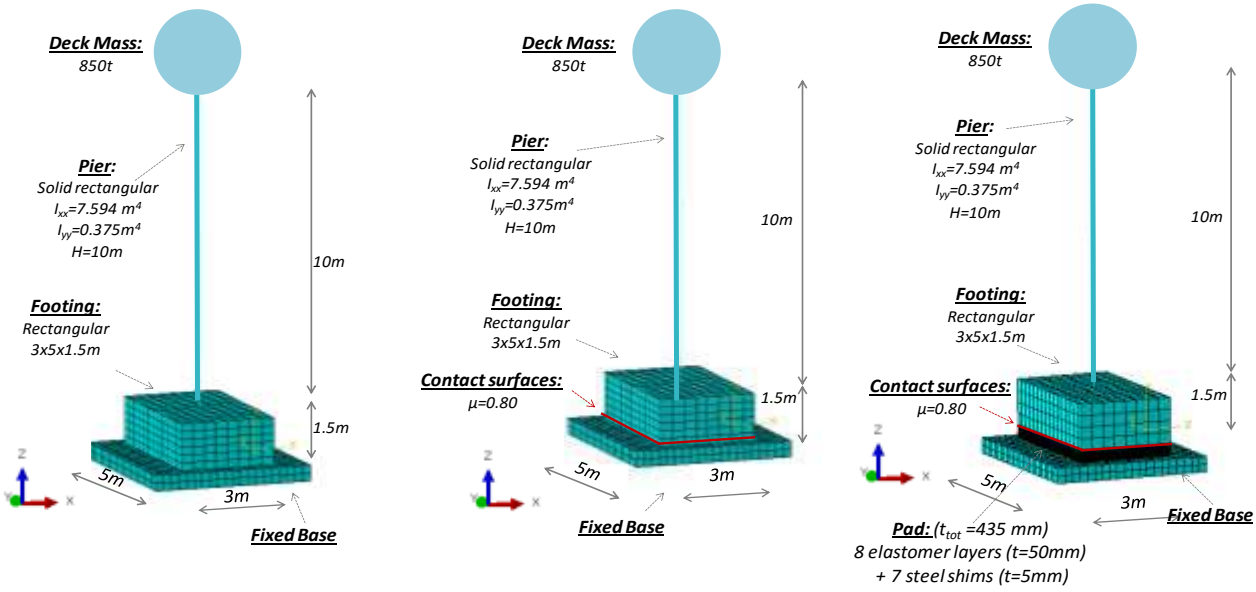

Fig 2 - 3D model in ABAQUS: (a) FX model, (b) C-C model and (c) C-P model.

3. Pier footing dimensions and design of the elastomeric pad

The design of the footing was based on design criteria that minimise the permanent deflection of the elastomeric pad under vertical loads (construction stage and serviceability), rectify the permanent dislocation (sliding) of the footing and limit the potential uplift of the foundation, so that the effective area of the foundation is at least 2/3 of the actual area of the foundation for all the design cases examined in this paper. Two alternative footing dimensions were examined: 3.5m x 6.0m and 3.0m x 5.0m. The footing was initially regarded as not slipping on the elastomeric pad and subsequently as sliding with a coefficient of friction. Thus different dimensions were checked for variable pier drifts ranging from 1% to 5%, different elastomeric pad properties and designs (soft and hard elastomer with or without reinforcing steel plating). Thus the foundation: (a) promotes rocking; (b) maximum uplift of the footing for the maximum design drift is controlled and as such this uplift does not cause eccentricity larger than 1/3 of the footing longitudinal dimension (c) the initial deflection (hypothetical settlement) of the pad is controlled. Different elast omer properties were analysed to design the high damping rubber isolator. For all material models checked the initial stiffness is mu1=0.41 and alpha1=1.6, the post-elastic stiffness is mu2=0.0012 and alpha2=6.2, based on [15] whilst values of the stress scaling factor SS of 1.6, 2.4 and 3.2 were analysed. The results presented in this paper refer to the SS=1.6 only. The preliminary design of the pad showed that a total thickness of the elastomer of 435mm is adequate to both minimise the initial deflection of the pad and to control successfully the uplift of the foundation for drifts 2 to 3%. The selected elastomeric pad consists of 8 layers of elastomer with thickness equal to 50mm each and 7 steel shims with thickness of 5mm. It is also noticeable from Fig. 3 that the smaller the foundation dimensions the larger the initial deflection of the pad and hence the smaller the uplift observed during the earthquake excitations.

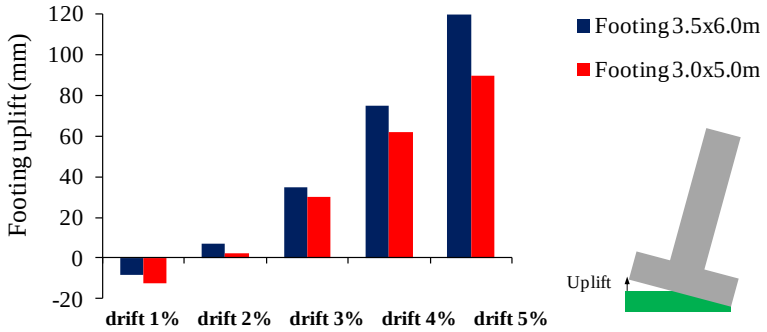

Fig 3 - Uplift of the footing for drifts of 1 to 5% for a pad thickness of 400mm.

4. Longitudinal period of the rocking pier models

In this section, the longitudinal response period of the CC and the CP model is estimated. Displacement along x-x axis is imposed on top of the pier and subsequently the pier model is left free to oscillate for 10 s. Restraint has been imposed at the bottom of the footing to prohibit the sliding between the footing and the concrete base or pad. During the oscillation, a number of non-linearities that affect the response of the CC and CP pier modes were taken into account. In particular the period and the damping ratio of the systems were estimated accounting for: (i) the contact effects between the surfaces, (ii) the friction forces, (iii) the damping of the materials i.e. concrete and elastomeric pad and, (iv) the plasticity of the materials. Fig.4 illustrates the time history of the horizontal displacement at the top of the pier during the oscillation for the CC and CP pier models. The damping ratio of the CC and the CP models was evaluated for small to large drifts ranging from 1% to 10%. The models were subjected to a target displacement of the pier top, corresponding to the aforementioned drifts, and subsequently they were left free to oscillate. The CC model oscillation was damped due to the collisions and sliding of the footing on the concrete sub-base. It was found that the total damping ratio was 3.8% when 10% drift was considered. The sources of dissipation of the CP model were the contact effects between the footing and the pad which yield a damping ratio of 2.1%. The elastomeric pad offered additional dissipation due to its hysteretic behaviour (another 9%), thus the total damping ratio of the CP model was found to be 11.1% for a drift of 10%, which is substantially higher than the one estimated for the CC pier model. In addition, the fundamental natural period of the CP model is 1.13 s, while the corresponding period of the CC model is initially 1.0 s and gradually reduces during free oscillations. In addition, permanent displacements on top of the pier were observed on the CC model, which reflects the potential of sliding for piers rocking on concrete surfaces.

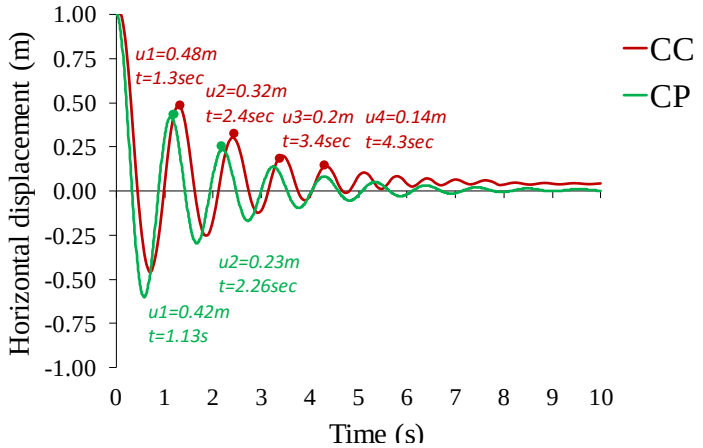

Models	Period T (s)
FX	0.51
CC	1.0 to 0.6
CP	1.13

Fig 4 - Identification of the periods of the C-C and the C-P model.

5. Comparison between models response to real earthquake excitations

The FX, the CC and the CP pier models were analysed for seven real accelerograms compatible to ground Type C-dependent Eurocode 8-1 elastic spectra. The peak ground accelerations selected were 0.30 g and 0.60 g to

represent medium and high seismic excitations. The response spectra of the analysed accelerograms are shown in Fig. 5. Accelerations are imposed at the base of the model, which is free to move along x-x axis. The duration of all the time history analyses is 35sec.

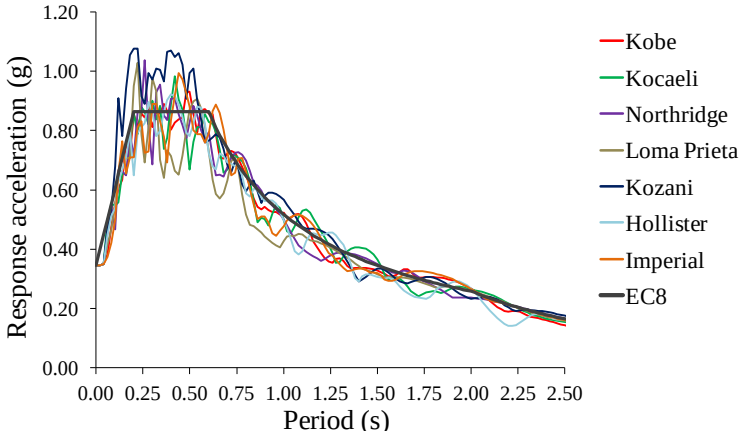

Fig.5- Response spectra of accelerograms compatible to ground Type C-dependent Eurocode 8-1 elastic spectra (PGA = 0.30 g).

Table 1 shows the mean values of the responses of the pier models analysed. The mean values were calculated based on the seven acceleration time histories for PGA of 0.30g and 0.60g. The values given on Table 1 are not simultaneous.

With regard to footing uplift, the CC model exhibited a mean uplift displacement of 26mm and 37mm for drifts of 0.88% and 1.7%, whilst the CP model either exhibited no uplift or a minor uplift of 2mm when the drift was 2.35%. It is noted that the CP model, which is more flexible than FX and CC models, which exhibited a mean drift of 1% and 2.4% for PGAs of 0.3 and 0.6 g correspondingly.

The benefits of the rocking CC and CP and can be observed on the basis of reductions of the bending moments and shear forces. In particular, the bending moments of the rocking CC and CP piers are reduced by approximately 15% and 26% for a PGA of 0.30g. Similarly, the shear forces are reduced by 45% and 64% correspondingly. Significant differences between the CC and CP pier models were observed with regard the axial load. In particular, the collision of the foundation of the CC system on the concrete sub-base causes a significant fluctuation of the axial load. As a result, the axial load of the CC model is up to 2.5 times larger than the axial load of the CP model. It is also noted that the axial load of the CP model is approximately equal to the one of the model with the fixed base (FX), indicating that the axial load is not fluctuating during the earthquake excitation. It is also noteworthy that the fluctuation of the axial load on the pier CC may lead in some cases to tension. This case was observed for the PGA of 0.6 g. This unexpected result was then verified by additional analysis of the results. The distribution of stresses revealed that when the pier footing pounds on the stiff concrete sub-base the deck is already uplifted. As a result, when the footing tents to return to its original position due to the recentering pounding force, it pulls down the pier and the deck, with the latter having an inertia mass that resists momentarily to this movement. This inertia force induces axial tension within the pier, which is reflected by the positive values in Table 1.

With regard to displacements of the deck, it was found that the displacements were increased on the CC and the CP pier models, as the mean deck displacement of the FX system is 59mm whilst the displacements of the CC and CP systems are 88 and 106 mm, i.e. 49% and 79% larger than the one of the FX pier. For the PGA of 0.6 g the bending moments of the rocking CC and CP piers are reduced by 26% and 37% correspondingly. Similarly, the shear forces are reduced by 60% and 78%.

The comparison between the two different rocking systems CC and CP showed that the pier rocking on the elastomeric pad reduces both the bending moments and shear forces more effectively (up to 12% and 35% respectively).

Table 1 - Average of the maximum values of seismic demand for the three models for PGA 0.30g and 0.60g

	PGA 0.30g			PGA 0.60g		
	fixed base FX	**concrete to concrete CC**	**concrete to pad CP**	**fixed base FX**	**concrete to concrete CC**	**concrete to pad CP**
horizontal movement at pier top (mm)	59	88	106	125	170	235
footing uplift (mm)	-	26	-	-	37	2
axial forces (kN) max /min	-8832/-8740	-21714/-180	-8710/-8645	-8950/8853	-31246/+900	-8870/-8795
shear force (kN)	7846	4334	2816	14282	5592	3182
bending moment at pier bottom (kN·m)	36256	30968	27207	57990	42859	36506

Fig. 6 illustrates the results for the Loma Prieta accelerogram scaled to a PGA of 0.30g, while Fig. 7 shows the results for the same earthquake scaled to 0.60g. These figures illustrate ttime histories of (a) the horizontal displacement at pier top, i.e. the longitudinal deck displacement, (b) the vertical displacement of the pier top with regard to its position after the imposition of the self-weight, (c) the vertical displacement of the footing for the CC model at three locations, i.e. left, middle and right side of the footing, (d) the vertical displacement of the footing for CP model, (e) the axial forces of the pier, (f) the axial forces of the pier normalised to the self-weight *W* pier i.e. N/W, where W includes the weight of deck, pier and footing, (g) the shear forces of the pier, (h) and the shear force normalised to the self-weight Q/W and (i) the bending moment of the pier bottom and (j) the normalised bending moment M/Q**k***h*, where *k* has a value 0.5 for the FX model, which was considered as a clamped-clamped column, while *k*=0.7 for CC and CP, as the latter models were assumed to respond as clamped-pinned columns, and *h* is the pier height.

Figure 6a shows that the displacements are increased when the CC and the CP models were considered, with the concrete-on-pad model exhibiting the largest movements. Figure 6b shows that the rocking pier top exhibits negligible vertical displacements under the seismic excitations, when the pier is either fixed at its base (FX) or when the footing is rocking on the elastomeric pads (CP). On the contrary the vertical displacements of the deck are reaching values of 20mm on the CC pier model. The latter displacements are considered to be detrimental for the deck if the latter is prestressed, as they might cause cracking of the deck and potential severe fluctuation of the prestressing stresses. Further investigation is required to identify the criticality of the aforementioned vertical movements of the CC pier model.

With regard to vertical footing displacements, the CC pier model was found to exhibit a maximum of 37mm uplift at the edges of its foundation, indicating a clear separation of the footing from the concrete sub-base. Notably Fig 6b and 6c show identical vertical displacements for the vertical displacement of the pier top and the centre of the footing for the CC pier model. The latter observation can be understood in light of the great axial stiffness of the pier. Contrarily, the CP pier model induced an initial pre-compression of the pad of 33.3 mm, which essentially cancels any uplift of the foundation at least for the PGA of 0.30 g. As a result, the rotations of the footing occur within the elastomer and no loss of contact was observed for the CP model.

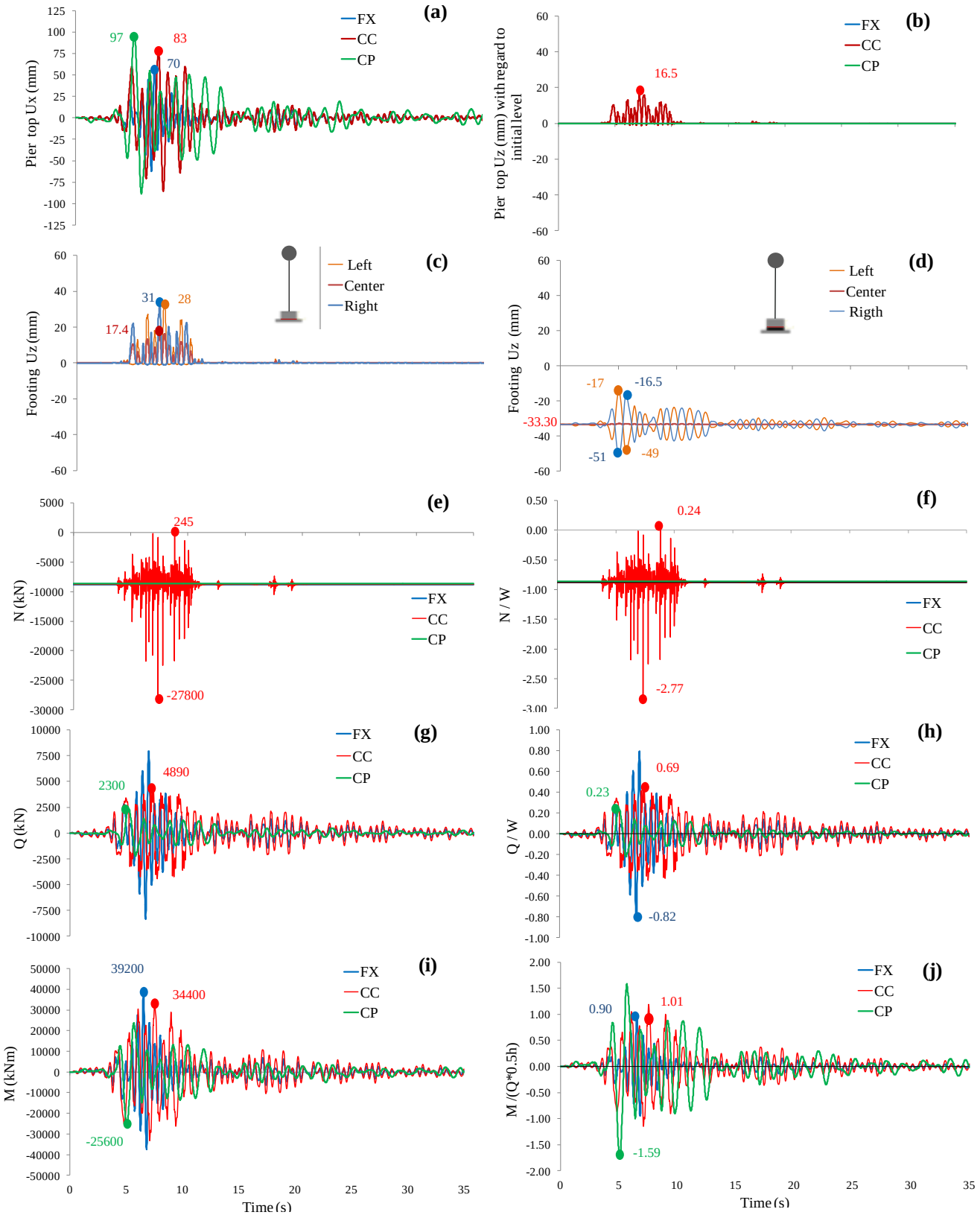

Fig 6 - Time histories of (a) horiz. displ. pier top, (b) vertical displ. pier top, (c) the vertical displ. of footing for CC, (d) the vertical displ. of footing for CP, (e) axial force of pier, (f) axial force normalised to the self-weight N/W, (g) shear forces of pier, (h) shear force normalised to self-weight Q/W (i) bending moment of pier bottom (j) normalised bending moment M/Q*k*h, for the real acceleration of Loma Prieta (Pga 0.3g).

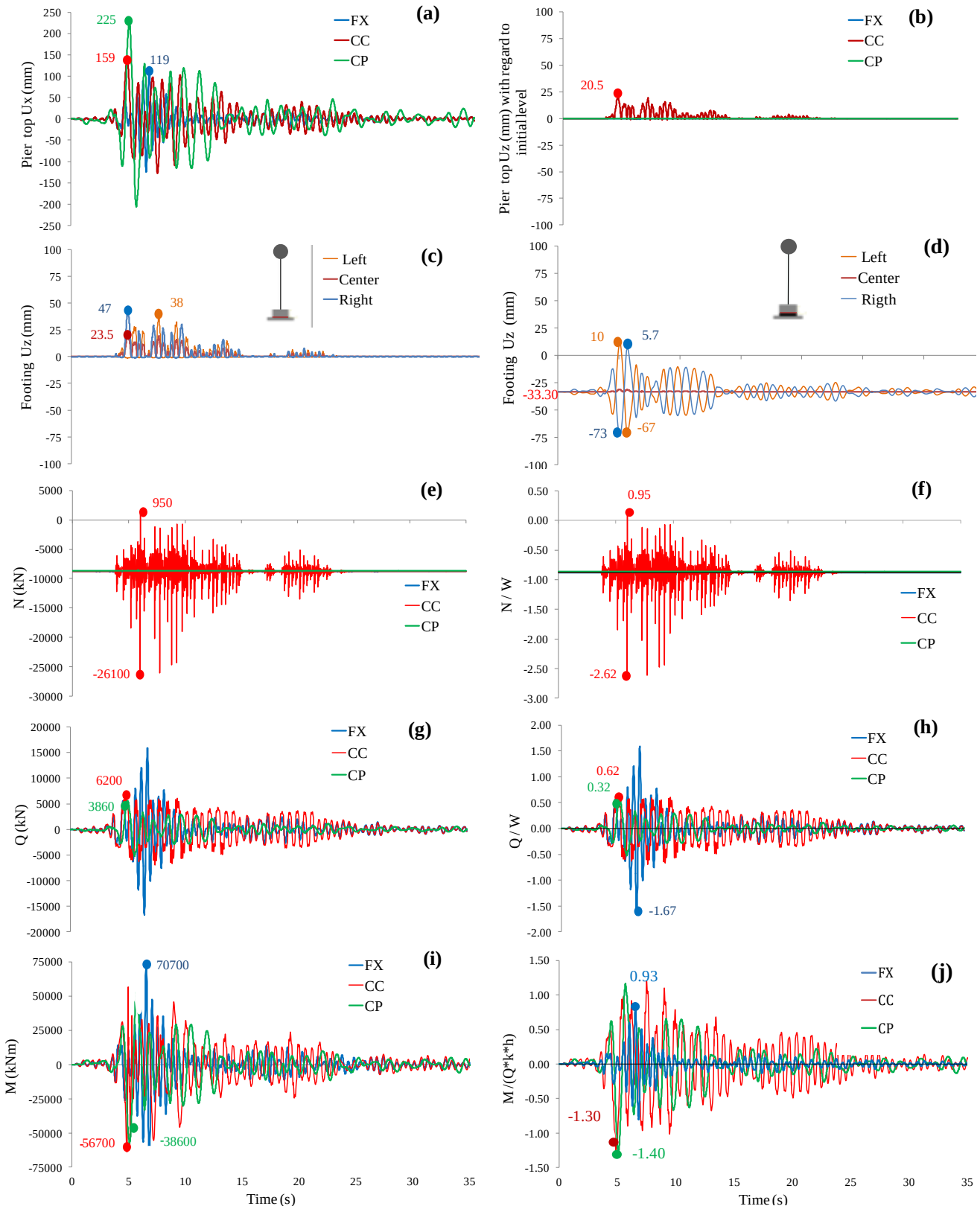

Fig 7 - Time histories of (a) horiz. displ. pier top, (b) vertical displ. pier top, (c) the vertical displ. of footing for CC, (d) the vertical displ. of footing for CP, (e) axial force of pier, (f) axial force normalised to the self-weight N/W, (g) shear forces of pier, (h) shear force normalised to self-weight Q/W (i) bending moment of pier bottom (j) normalised bending moment M/Q*k*h, for the real acceleration of Loma Prieta (PGA 0.6g).

An interesting result of this investigation is the axial load of the pier. Figures 6e and 6f show the values of axial load and also the values of the same load normalised with respect the self-weight of the pier model. It is observed that the FX and the CP model respond with axial loads that exhibit negligible fluctuations. Contrarily, the CC model, where the pier footing rocks on the concrete sub-base is subjected to large pounding forces, which tend to restore the position of the pier and also dissipate seismic energy. However, these pounding forces induce momentarily large tensile loads within the pier and hence the significant fluctuations of the axial load of the pier, an effect that was described above in detail and is shown in Table 2 and Figure 8. This is an undesirable effect that may require attention under design situations as the axial load alters the capacity of the pier.

Regarding the shear forces and the bending moments within the pier, Fig. 6j to 6j show that these loads are reduced when the CC or the CP model is considered instead of the FX model. Also, the CP pier model was evidently more efficient in reducing the bending moments and shear actions of the piers for all the cases studied herein.

The results are pretty much the same for the highest PGA of 0.6 g. What differs in this case is the relatively large uplift displacements of the footing of the CC, the marginal uplift of the footing of the CP pier model, and the extremely high fluctuation of the axial load of the CC pier model, that lead to tensile loads within the pier.

A clearer interpretation of the severe fluctuation of the axial load of the CC pier model can be provided with the help of Table 2 and Figure 8, which show the response of the CC pier model at time t=8.82 s, i.e. at the time when the tensile load was developed within the pier. The results correspond again to the scaled Loma Prieta earthquake for PGA 0.3 g. Both the table and the figure provide evidence of the mechanism described above, i.e. the pounding forces induce large tensile stresses within the footing. The latter tends to recentre and hence pulls the deck downwards, as a result tension is induced in the pier of the CC model.

Table 2. The response of the CC pier model when tensile axial force is developed (t=8.82sec)

response parameter	**value**
max horizontal deck displacement (mm) / drift %	83 / 0.83%
deck uplift Uz (mm)	+11
footing max uplift (mm)	30
axial forces (tensile) (kN)	244.87
shear force (kN)	1483
bending moment at pier bottom (kN·m)	6635

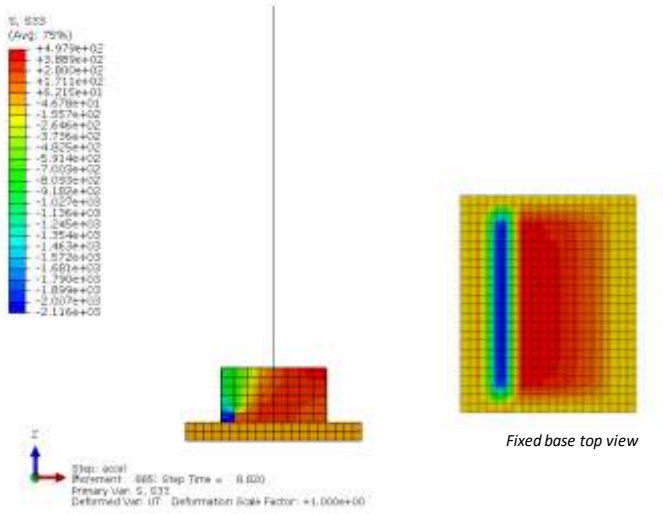

(a) (b)

Fig 8 - (a) Normal Stress on the footing and fixed base of CC model, (b) Normal on the top view of the fixed based for the real accelerogram of Loma Prieta at time step t=8.82sec.

6. Conclusions

The aim of this paper was to investigate realistic applications of rocking isolation for bridges. In doing so, means of additional dissipation were sought by using high damping rubber pads upon which the footing rocks. The footing was deliberately under-designed to promote rocking. The elastomeric pad was selected on the basis of design criteria to limit the initial pre-compression of the pad and to control the eccentricity of the pier vertical load under the target seismic displacements. Subsequently, three bridge pier models i.e. a fixed base (FX), a pier with a footing rocking on concrete (CC) and a pier with a footing rocking on elastomeric pads (CP) were modelled and analysed on ABAQUS. Material and geometric non-linearities were taken into account for all the analyses. Comparisons between the three model piers were performed on the basis of displacements and actions of the piers (axial, shear forces and bending moments). Based on the findings of this study the following conclusions were drawn:

1. Appropriate design of the elastomeric pad and the dimensioning of the rocking footing seem to provide adequate means of dissipation, with the main source of dissipation being the hysteresis of the elastomer. Indicatively, the CC model exhibited a damping ratio of 3.8% and this included the contact effects on the footing and the dissipation due to friction. The damping ratio of the CP pier model was found to be approximately 11% and this is mainly due to the dissipation capacity of the pad. Notably, elastomeric pads are designed to remain elastic, thus no replacement of the bearing is necessary after a strong earthquake motion.
2. Rocking isolation is beneficial as it reduces drastically the bending moments and the shear actions on the bridge piers. More specifically, the bending moments of the rocking CC and CP piers are reduced by approximately 15% and 26% correspondingly for a peak ground acceleration (PGA) of 0.30g and by 26% and 37% for a PGA of 0.60g. The shear forces were also reduced drastically (45% and 64% for a PGA of 0.30g and by 75% and 78% for PGA of 0.60g).
3. The collision of the foundation of the CC pier model on the concrete sub-base causes a significant fluctuation of the axial load of the pier together with higher mode effects. As a result, the axial load of the CC model is up to 2.5 times higher than the axial load of the FX and the CP pier, whilst the vertical inertia of the deck that resists to the recentering of the pier might cause tension within the pier during earthquakes. On the other hand, the axial load of the pier rocking on the pad (CP) exhibited negligible fluctuations, like the FX pier model.

7. References

[1] US Department of Transportation, Federal Highway Administration (FHWA) (2014) Deficient Bridges by State and Highway System.

[2] Banerjee S, Chandrasekaran S, Venkittaraman A (2014): Optimal Bridge Retrofit Strategy to Enhance Disaster Resilience of Highway Transportation Systems, PSU-2012-01.

[3] Rodgers GW, Mander JB, Chase JG, Dhakal RP (2015): Beyond Ductility: Parametric Testing of a Jointed Rocking Beam-Column Connection Designed for Damage Avoidance, *J. Struct. Eng., 10.1061/(ASCE)ST.1943-541X.0001318 , C4015006*.

[4] Marsh et al. (2011): Application of Accelerated Bridge Construction Connections in Moderate-to-High Seismic Regions, National Cooperative Highway Research Program, (*NCHRP report 698*).

[5] Kelly JM, Konstantinidis D (2011) Mechanics of rubber bearings for seismic and vibration isolation. Wiley: Chichester.

[6] Mergos PE, Kawashima K (2005): Rocking isolation of a typical bridge pier on spread foundation. *Journal of Earthquake Engineering*, **9**, 395-414. doi: 10.1142/S1363246905002456.

[7] Makris N, Vassiliou MF (2013): Planar rocking response and stability analysis of an array of free-standing columns capped with a freely supported rigid beam. *Earthquake Engng. Struct. Dyn.*, **42**: 431-449. doi: 10.1002/eqe.2222.

[8] Gelagoti F, Kourkoulis R, Anastasopoulos I, Gazetas G (2012): Rocking isolation of low-rise frame structures founded on isolated footings. *Earthquake Engng. Struct. Dyn.*, **41**, 1177–1197.

[9] Gazetas G (2014): 4th Ishihara lectrure: Soil-foundation-structure systems beyond conventional seismic failure thresholds. *Soil Dynamics and Earthquake Engineering*, **68**, 23-39.

[10] Anastasopoulos I, Drosos V, Antonaki N (2015). Three storey building retrofit rocking isolation versus conventional design. *Earhtquake Engineering and Structural Dynamics*, 44, 1235-1254.

[11] Abaqus Simulia, (2012). Analysis User's Manual Volume IV. Analysis User's Manual Volume IV . Providence: Dassault Systèmes.

[12] Mitoulis S, Palaiochorinou A, Georgiadis I, Argyroudis S (2016): Extending the application of integral frame abutment bridges in earthquake prone areas by using novel isolators of recycled materials, *Earthquake Engineering and Structural Dynamics (accepted).*

[13] Ogden WR (1972): Large Deformation Isotropic Elasticity–On the Correlation of Theory and Experiment for Incompressible Rubberlike Solids. *Proceedings of the Royal Society of London. Series A, Mathematical and Physical Sciences*, **326** (1567), 565–584, The Royal Society.

[14] Ohsaki M (2015): Finite-Element Analysis of Laminated Rubber Bearing of Building Frame under Seismic Excitation. *Earthquake Engineering & Structural Dynamics*.

[15] Dassault Systèmes, 2014. Computer Program ABAQUS/CAE. Providence, RI.

[16] Bergström JS, Boyce MC (1998): Constitutive Modeling of the Large Strain Time- Dependent Behavior of Elastomers. *Journal of Mechanics Physics Solids*, **46**, 931- 954.